EFFECT OF TITANIUM CARBIDE ADDITION ON THE WORKABILITY BEHAVIOR OF POWDER METALLURGY ALUMINUM PREFORMS DURING HOT DEFORMATION

S. Narayan *, A. Rajeshkannan

School of Engineering and Physics, Faculty of Science, Technology & Environment, The University of the

South Pacific, Laucala Campus, PO Box 1168, Suva, FIJI.

*e-mail: narayan_su@usp.ac.fj

Abstract. Experimental investigation has been carried out to evaluate the effect of titanium carbide (TiC) addition on the composite aluminium preforms. The hot upsetting of the composite aluminium preforms with varying TiC contents, namely, 1%, 2%, 3% and 4%, and different aspect ratios, namely, 0.2, 0.4 and 0.6, was carried out and the workability behavior of the same was determined. The influence of TiC addition, in the aluminium composite, on the relative density (R), stress ratio parameters, $\sigma_\theta/\sigma_{eff}$, σ_m/σ_{eff} and σ_z/σ_{eff} and formability stress index was studied. The effects of initial preform geometry and initial theoretical density on the workability behavior have been studied.
Keywords: workability; stress ratio parameter; formability stress index; relative density; triaxial stress.

1. Introduction

Today, many researchers are working on producing frontier materials in this research field that will benefit our society in one way or another. Technological advancement and improved materials in terms of cost, manufacturability and strength are not the only concern today unlike in the traditional days. One of the most important issues today is global warming, climate change issues, ecological, etc. and for any developments in technology and materials there is need to capture these important issues. One of the manufacturing routes so called powder metallurgy manufacturing route is considered to be green materials processing route [1] in comparison to traditional or conventional casting materials processing route. Some of the merits of powder metallurgy manufacturing route over traditional casting process is that energy consumption is reduced by 50%, very little fumes & chemicals emitted in the atmosphere, use of re-cycled metals, the emerging consumer preferences for green products, and increasing disposal costs due to scarcity of land fields [1-2]. Every manufacturing process has its own merits and demerits and one of the main concerns with powder metallurgy processing route is that it produces parts with residual porosity. Hence, high strength applications of powder metallurgy parts are limited in the practical world. Secondary operations such as pressing or repressing, powder extrusion, powder rolling and infiltration etc., can be employed to increase the strength of the powder metallurgy materials by eliminating the residual porosity [3]. Aluminium metal matrix composites are highly used in high strength industrial application due to low specific density, high strength, good wear resistance, low thermal expansion coefficient, etc [4, 5]. Sahin [5] studied the preparations of metal matrix composites by developing the method and some properties (hardness, tool wear in turning, density and porosity) of SiC

particles reinforced aluminium alloy composites. It is shown that metal matrix composites of 10 and 20 wt.% SiC particles can be produced successfully using molten metal mixing method. Titanium carbide based composites are currently used in high strength application where wear and corrosion are the main mode of failure. Titanium carbide particulates are extremely hard and the improvement in wear resistance and reduced corrosion rate is expected [6]. Narayanasamy et al. [6] studied the effect of TiC addition of the densification behaviour on the composite steel preforms. The two composites prepared via P/M route and analyzed were Al-3%TiC and Al-4%TiC. Titanium and its alloy are developed because of its low cost and good performance. Liu et al. [7] has shown that low cost P/M Ti alloys and their composites with their attractive properties can be produced through a single primary P/M processing route, although secondary treatments are required for high strength applications. Titanium carbide based composites with nickel alloys and iron alloys are currently used in high performance applications [6, 8].

Workability is an important parameter that needs to be studied while powder metallurgy preforms are subject to secondary deformation. During secondary deformation powder metallurgy preforms has substantial material flow in the lateral direction due to induced height strain. During lateral flow of material or deformation, apart from pore closing mechanism, the pores also elongate in the lateral direction. Workability is a measure of the extent of deformation that a material can withstand the induced internal stresses of forming prior to failure. Workability characteristics are not only dependent on the material but also by several forming parameters such as stress and strain rate, porosity, friction, temperature, etc [9-11]. To investigate the workability criteria of the material, ductile fracture criterion for ductile fracture must be established as workability of any material depends mainly on the amount of ductile fracture present in the material. There are many theories developed and verified with experimental results in study the workability behavior of powder metallurgy materials. Shima and Oyane [12], Gurson [13] and Doraivelu et al. [14] proposed a plasticity theory for porous materials, continuum theory of ductile rupture considering yield criteria for porous material and a new yield criterion for porous material validating it using experiments and simulations, respectively. Narayansamy et al. investigated the working behavior of Al-Al$_2$O$_3$ composites under various stress state conditions, namely uniaxial, plane and triaxial stress states. The effects of different curve fitting techniques, aspect ratio, and initial preform density on the workability criteria were presented [15]. They used a generalized yield criterion considering an-isotropic parameters for powder metallurgy metals which was earlier proposed by Narayansamy et al. [16] with a new flow rule with an-isotropic parameters for porous metals. Rahman and El-Sheikh [10] proposed the stress formability criteria (β) for describing the effect of mean stress and the effective stress by employing theories proposed by Kuhn-Downey [17] and Whang-Kobayashi [18]. Gouveia et al. [19] conducted experiments on P/M compacts of several geometries and reported that the initiation of the ductile fracture can be predicted. The attention on the hoop stress, hydrostatic stress and axial stress behaviour of any P/M materials is much required for any forging processes and Narayanamurti et al. [20] presented some of the important criteria generally used for the prediction of ductile fracture. Crack appearance on the powder metallurgy preform can be avoided by careful selection of process parameters and deformation process. Thus, the present investigation is aimed to establish the workability limit under triaxial stress state condition of powder metallurgy preforms of Al-1%TiC, Al-2%TiC, Al-3%TiC, and Al-4%TiC experimentally and to establish the technical relationship that exists between the characteristics of axial stress, hoop stress, hydrostatic stress, effective stress and formability stress index with respect to true height strain and densification.

2. Experimental details

Aluminium powder of less than or equal to 150 μm and titanium carbide powder of less than or equal to 50 μm were mixed to obtain the alloy of Al-1%TiC, Al-2%TiC, Al-3%TiC, and Al-4%TiC via ball milling. The ball mill was operated for 2 hours at 200 rpm to get a homogenized mixture. The sieve analysis of pure aluminium powder and powder characterization of aluminium powder and its respective blends are given in Tables 1 and 2, respectively.

Table 1. Sieve size analysis of aluminium powder.

Sieve size (µm)	250	+200	+150	+100	+75	+45	-45
Wt % Ret.	0.2	0.3	16.3	55.3	9.5	7.9	10.5

Table 2. Characterization of aluminium powder and its blends.

Si. No.	Property	Al	Al-1%TiC	Al-2%TiC	Al-3%TiC	Al-4%TiC
1.	Apparent Density (g/cc)	1.091	1.133	1.186	1.247	1.280
2.	Flow rate, (s/50g) by Hall Flow Meter	87.306	86.801	85.202	83.086	81.478
3.	Compressibility (g/cc) at pressure of 130±10MPa	2.356	2.342	2.325	2.302	2.280

The powders with different aspect ratios and different initial theoretical density were then compacted using 100 tons capacity hydraulic press. The compaction pressure was controlled so as to obtain an initial theoretical density of 0.82 ± 0.01 and 0.86 ± 0.01. The compacts were coated on all surfaces with ceramic coating. This coating was allowed to dry for a period 12 hours at normal atmospheric conditions. Recoating was employed to the preforms in the direction 90° to that of the earlier coating. Again the compacts were allowed to dry for a period of 12 hours. The coating was applied to avoid oxidation of compacts.

The ceramic coated compacts were sintered in an electric muffle furnace at a temperature of 220°C for 30 minutes and then the temperature was increased to 594°C. At this temperature the compacts were sintered for a further period of 60 minutes. After the sintering operation, the preforms were upset forged at a temperature of 594°C to the different levels of height strain. The forging operation was carried out with no lubricant. The density of forged preforms was determined using Archimedes principle. After the above mentioned forging schedule, the dimensions, namely, the height of forged specimen (h_f), the contact diameter (D_{c1} and D_{c2}) of top and bottom surfaces and the bulged diameter (D_b), were measured. Initial dimensions of the specimen (initial height h_o, initial diameter D_o) and the initial preform density were measured for each preform before conducting the experiment.

3. Theoretical analysis

Using the mathematical expressions, the various upsetting parameters of upsetting were determined under uniaxial stress state condition, plane stress state condition and triaxial stress state condition.

3.1. Uniaxial stress state condition. According to Abdel-Rahman and El-Sheikh [10], the expression for true axial stress and mean stress for powder metallurgy materials are as follows:

$$\sigma_z = \frac{load}{contact\ surface\ area} = -\sigma_{eff}, \quad \sigma_r = \sigma_\theta = 0 \tag{1}$$

$$\sigma_m = \left(\frac{\sigma_z}{3}\right) = -(\sigma_{eff}/3) \tag{2}$$

and the expression for the axial strain can be written as follows:

$$\varepsilon_z = -\varepsilon_{eff} = \ln\left(\frac{h_f}{h_o}\right) \tag{3}$$

and true hoop strain is

$$\varepsilon_\theta = \varepsilon_r = \ln\left(\frac{D_f}{D_o}\right), \tag{4}$$

where h_o is the initial height of the preform; h_f the forged height of the preform; D_f the contact diameter after deformation of the preform; D_o the initial diameter of the preform.

3.2. Plane stress state condition. According to Narayansamy et al. [9, 15], the hoop strain which includes the forged bulged diameter (Db) and forged contact diameter (Dc) can be expressed as follows

$$\varepsilon_\theta = ln\left[\frac{2D_b^2 + D_c^2}{3D_o^2}\right] \tag{5}$$

and state of stress can be written as

$$\sigma_{eff} = (0.5 + \alpha)[3(1 + \alpha + \alpha^2)]^{0.5}\sigma_z, \tag{6}$$

where α is the Poisson's ratio $= (\varepsilon_\theta/2\varepsilon_z)$

The hoop stress can be written as ($\sigma_r = 0$ at the free surface in plane stress state condition)

$$\sigma_\theta = \left[\frac{1+2\alpha}{2+\alpha}\right]\sigma_z \tag{7}$$

and the hydrostatic stress is

$$\sigma_m = \frac{\sigma_\theta + \sigma_z}{3} \tag{8}$$

The various stress ratio parameters can be written as follows form Equations 6-8:

$$\frac{\sigma_{eff}}{\sigma_z} = (0.5 + \alpha)[3(1 + \alpha + \alpha^2)]^{0.5} \tag{9}$$

$$\frac{\sigma_\theta}{\sigma_z} = \left[\frac{1+2\alpha}{2+\alpha}\right] \tag{10}$$

$$\frac{\sigma_m}{\sigma_z} = \frac{1}{3}\left(1 + \frac{\sigma_\theta}{\sigma_z}\right) \tag{11}$$

The formability stress index proposed by Vujovic and Shabaik [21] stating the importance of the spherical component of stress state on fracture can be expressed as

$$\beta = 3\left[\frac{(\sigma_m/\sigma_z)}{(\sigma_{eff}/\sigma_z)}\right] \tag{12}$$

3.2. Triaxial stress state condition. According to Narayansamy et al. [6], the state of stress in a triaxial stress condition is given by

$$\alpha = \frac{d\varepsilon_\theta}{d\varepsilon_z} = \frac{(2+R^2)\sigma_\theta - R^2(\sigma_z + 2\sigma_\theta)}{(2+R^2)\sigma_\theta - R^2(\sigma_z + 2\sigma_\theta)} \tag{13}$$

Using Eq. (13) for the values of Poisson's ratio (α), relative density (R) and axial stress (σ_z) the hoop stress (σ_θ) under triaxial stress state condition can be determined as given below:

$$\sigma_\theta = \left[\frac{2\alpha + R^2}{2 - R^2 + 2R^2\alpha}\right]\sigma_z, \tag{14}$$

where $\alpha = \frac{d\varepsilon_\theta}{d\varepsilon_z}$

and relative density (R) in important in finding the hoop stress.

Further, rearranging Equation 14

$$\frac{\sigma_\theta}{\sigma_z} = \left[\frac{2\alpha + R^2}{2 - R^2 + 2R^2\alpha}\right] \tag{15}$$

Under triaxial stress state cylindrical coordinates, the hydrostatic stress can be written as follows assuming $\sigma_\theta = \sigma_r$:

$$\sigma_m = \frac{\sigma_r + \sigma_\theta + \sigma_z}{3} = \frac{2\sigma_\theta + \sigma_z}{3} \tag{16}$$

Further, rearranging Equation 16

$$\frac{\sigma_m}{\sigma_z} = \frac{1}{3}\left(1 + \frac{2\sigma_\theta}{\sigma_z}\right) \tag{17}$$

The effective stress can be written as explained elsewhere [22]

$$\frac{\sigma_{eff}}{\sigma_z} = \left[\frac{1 + 2(\sigma_\theta/\sigma_z)^2 - R^2\left(2(\sigma_\theta/\sigma_z) + (\sigma_\theta/\sigma_z)^2\right)}{2R^2 - 1}\right]^{0.5} \tag{18}$$

The stress formability factor under triaxial stress state condition is given as

$$\beta = 3\left[\frac{(\sigma_m/\sigma_z)}{(\sigma_{eff}/\sigma_z)}\right] \tag{19}$$

The stress formability factor as expressed in Eq. (19) is used to describe the effect of mean stress and the effective stress on the forming limit of P/M compacts in upsetting.

Different stress ratio parameters, namely, $(\sigma_\theta/\sigma_{eff})$, (σ_m/σ_{eff}) and (σ_z/σ_{eff}) are expressed as follows:

$$\frac{\sigma_\theta}{\sigma_{eff}} = \left(\frac{\sigma_\theta/\sigma_z}{\sigma_{eff}/\sigma_z}\right) \tag{20}$$

$$\frac{\sigma_m}{\sigma_{eff}} = \left(\frac{\sigma_m/\sigma_z}{\sigma_{eff}/\sigma_z}\right) \tag{21}$$

$$\frac{\sigma_z}{\sigma_{eff}} = \left(\frac{1}{\sigma_{eff}/\sigma_z}\right) \tag{22}$$

4. Results and discussion

A plot has been presented as shown in Fig. 1 between true height strain and percentage fractional theoretical density for Al-2TiC preforms for two different initial aspect ratios, namely, 0.20 and 0.60, these plots being drawn for two different initial theoretical densities of 82% and 86%. From Fig. 1 it can be seen that there are two stages of deformation. During the initial stages of deformation the densification increases rapidly and thereafter the densification remains constant. Most of the pores are closed effectively during the first stage of deformation and thereafter the pores are elongated due to increasing material flow in the lateral direction before effective closure. For a given true height strain, the density attained by a lower aspect ratio preforms is higher in comparison to higher aspect ratio preforms. Further, the same is true for higher initial density preforms in comparison to lower initial density preforms. Lower aspect ratio preforms has lower pore bed height compared to higher aspect ratio preforms, hence, the density attained for any given height strain is higher for lower aspect ratio preform. It is impossible to achieve 100 percent density for powder metallurgy materials and during the initial stages of the deformation most of the pores are closed effectively, hence, lower aspect ratio and higher initial density preforms has high attained density for any given true height strain. A plot has been presented as shown in Fig. 2 between true height strain and percentage fractional theoretical density for various sintered aluminium composites with aspect ratio of 0.40 and initial theoretical density of 86%. From Fig. 2 it can be seen that for any given true height strain, the density attained by the preforms decreases as the percentage of titanium carbide particles (TiC) increases in the preforms, however, the fracture strain is increased as the TiC content in the aluminium composite increases. With increasing hard carbide particles in the preforms, the increasing lateral flow of the material is evident in Fig. 3 signaling the increasing strength of the preforms. Hence, more applied load is required for further deformation. Further, with the increasing smaller carbide particles in the preforms increases the number of smaller pores further delaying the densification rate with increasing carbide particles.
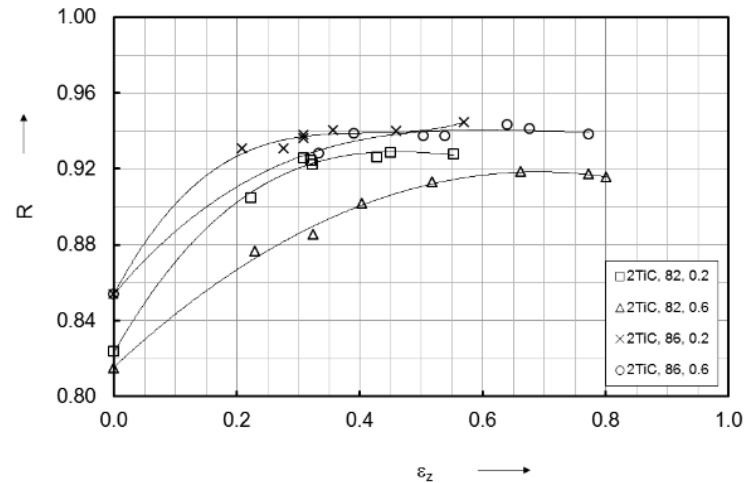
Fig. 1. Influence of aspect ratios and initial theoretical density on the relationship between percent theoretical density and true height strain of Al-2TiC.
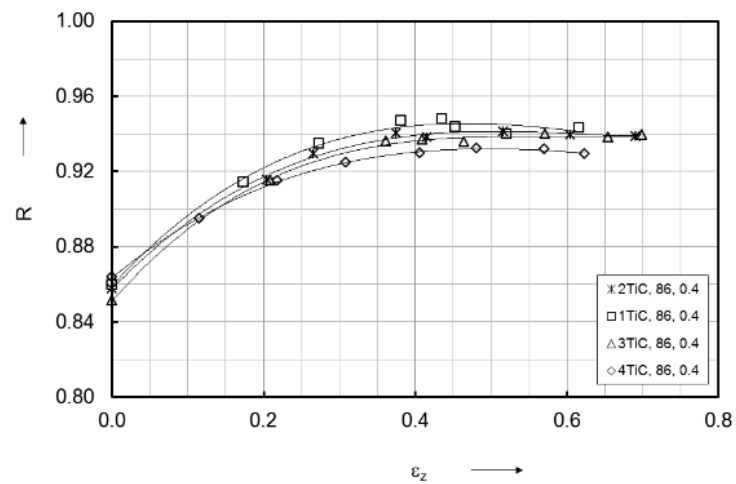

Fig. 2. Relationship between percent theoretical density and true height strain for various sintered aluminium composites.
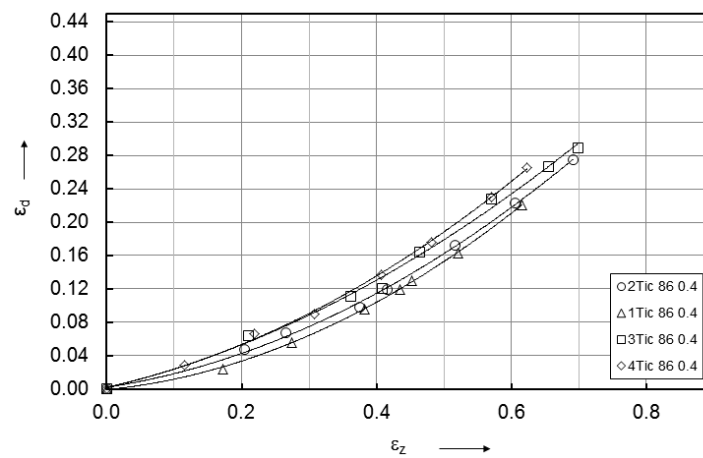

Fig. 3. Relationship between diameteral strain and true height strain for various sintered aluminium composites.

A plot has been presented as shown in Fig. 4 between true height strain and stress ratio parameter, $\sigma_\theta/\sigma_{eff}$, for Al-2TiC preforms for two different initial aspect ratios, namely, 0.20 and 0.60, these plots being drawn for two different initial theoretical densities of 82% and 86%. Further, a plot has been presented as shown in Fig. 5 between true height strain and stress ratio parameter, $\sigma_\theta/\sigma_{eff}$, for various sintered aluminium composites with aspect ratio of 0.40 and initial theoretical density of 86%. It can be seen from Figs. 4 & 5 that the hoop stress on the cylindrical preforms during hot deformation increases sharply to almost a maximum value with the increase in strain followed by attainment of steady state stress. The curves plotted in Figs. 4 & 5 clearly portrays the effect of initial relative density, geometry and percentage of TiC in the preforms on the maximum stress achieved for any given true height strain and the final steady state stress. As expected, the stress ratio parameter, $\sigma_\theta/\sigma_{eff}$, increases with increasing levels of strain and increasing initial theoretical density and decreasing aspect ratio. It is found that the stress ratio parameter, $\sigma_\theta/\sigma_{eff}$, decreases for any given true height strain as the TiC content in the aluminium composite is increased. To achieve same hoop stress in the aluminium composites with varying TiC contents, the higher TiC containing composite needs to be deformed more than the lower TiC containing composite. This suggests that the aluminium composite strength increases with the increasing TiC content in the composites. The same is true for stress ratio parameters σ_m/σ_{eff} and σ_z/σ_{eff} as seen in Figs. 6 & 7 as the difference between hydrostatic stress, hoop stress, and axial stress is literally nil against true height strain.
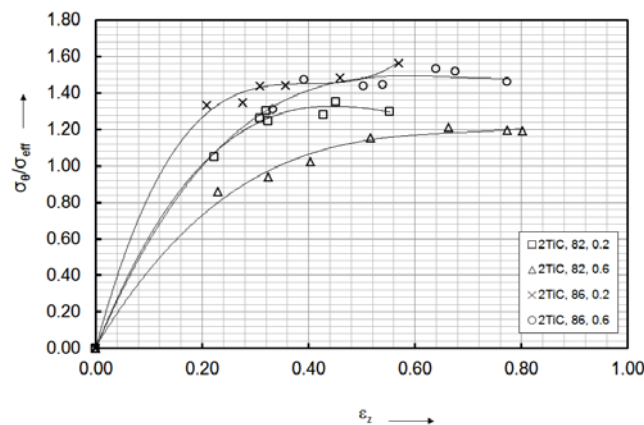

Fig. 4. Influence of aspect ratios and initial theoretical density on the relationship between stress ratio parameter, $\sigma_\theta/\sigma_{eff}$, and true height strain of Al-2TiC.
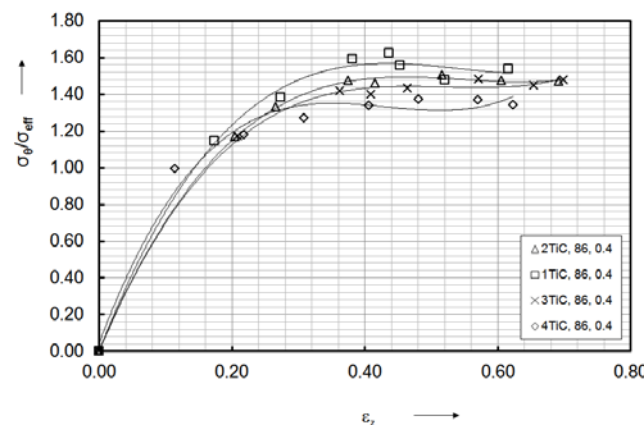

Fig. 5. Relationship between stress ratio parameter, $\sigma_\theta/\sigma_{eff}$, and true height strain for various sintered aluminium composites.
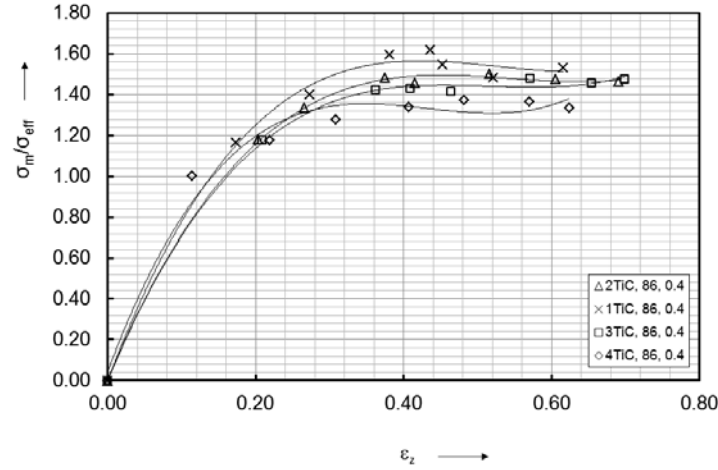
Fig. 6. Relationship between stress ratio parameter, σ_m/σ_{eff}, and true height strain for various sintered aluminium composites.
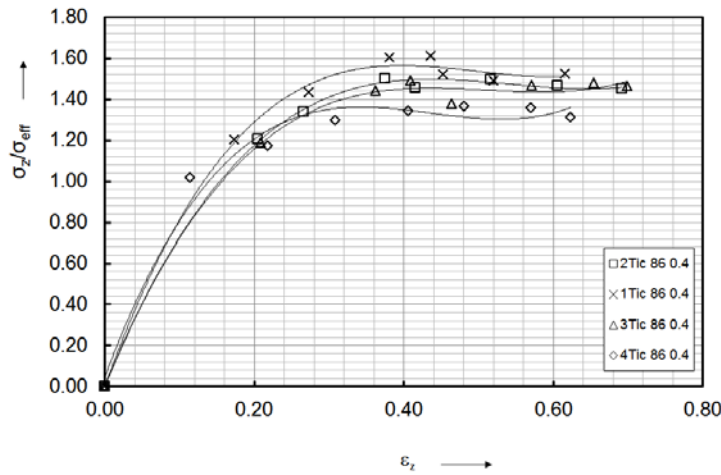

Fig. 7. Relationship between stress ratio parameter, σ_z/σ_{eff}, and true height strain for various sintered aluminium composites.

Figures 8 to 10 is drawn for hoop ($\sigma_\theta/\sigma_{eff}$), mean ($\sigma_m/\sigma_{eff}$), and axial ($\sigma_z/\sigma_{eff}$) stress ratios to that of relative density (R) respectively for various sintered aluminium composite with aspect ratio of 0.40 and initial theoretical density of 86% under hot upsetting of triaxial stress state condition. The stress ratio behavior of the composite plotted in Figs. 8 to 10 was found to be identical. It is noted that the effect of TiC content in the aluminium composite made zero impact on the stress ratio behavior. However, the highest stress ratio value obtained for the smallest percentage of TiC containing composite, which is true for all the stress ratio conditions. As the TiC percentage decreases in the aluminium composite, the maximum stress ratio parameters, ($\sigma_\theta/\sigma_{eff}$), ($\sigma_m/\sigma_{eff}$), and ($\sigma_z/\sigma_{eff}$) also decreases. Hence, Al-4TiC composite can be deformed further provided it is free of defects. Increasing the TiC particles in the preforms, increases chances of further deformation, promoting densification and strength in the composite. It is also noted that there is enhancement in the rate at which the stress ratio parameters increase as the densification progresses.
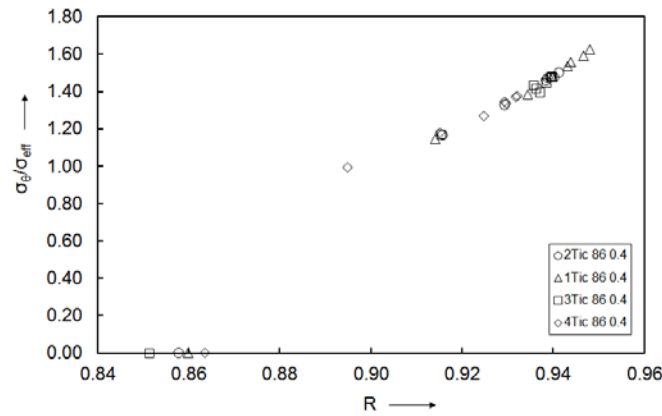
Fig. 8. Relationship between stress ratio parameter, $\sigma_\theta/\sigma_{eff}$, and relative density for various sintered aluminium composites.
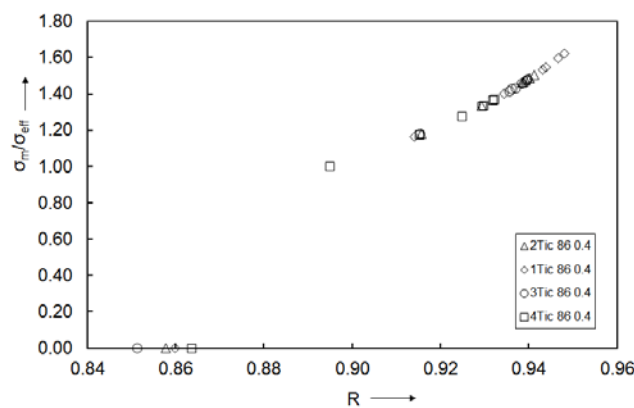

Fig. 9. Relationship between stress ratio parameter, σ_m/σ_{eff}, and relative density for various sintered aluminium composites.
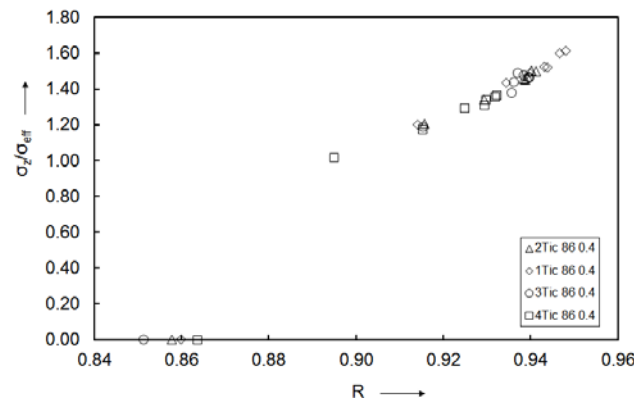

Fig. 10. Relationship between stress ratio parameter, σ_z/σ_{eff}, and relative density for various sintered aluminium composites.

A plot has been presented as shown in Fig. 11 between true height strain and formability stress index for Al-2TiC preforms for two different initial aspect ratios, namely, 0.20 and 0.60, these plots being drawn for two different initial theoretical densities of 82% and 86%. Further, a plot has been presented as shown in Fig. 12 between true height strain and formability stress index for various sintered aluminium composites with aspect ratio of 0.40 and initial theoretical density of 86%. It is observed that formability stress index varies with initial theoretical density, aspect ratio and percentage of TiC content in the preforms. The formability stress index increases with the increasing true height strain. Further, as the initial theoretical density

increases and aspect ratio decreases, the formability stress index also increases for any given true height strain. Also as the percentage of TiC increases in the preforms, the formability stress index decreases for any given true height strain. Formability stress index determines the fracture limit of the deforming material and it can be seen with the increasing percentage of TiC in the preforms, increasing pore bed height and decreasing initial theoretical density decreases the workability of the materials. With increasing smaller TiC hard carbide particles taking up space between Al particles in the preform increases the number of smaller pores giving rise to more lateral deformation (Fig. 3) which in turn reduces the formability of the material.
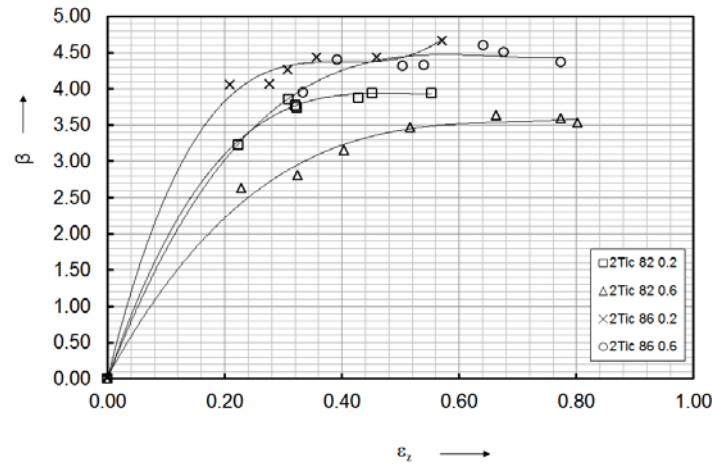

Fig. 11. Influence of aspect ratios and initial theoretical density on the relationship between the formability stress index and true height strain of Al-2TiC.
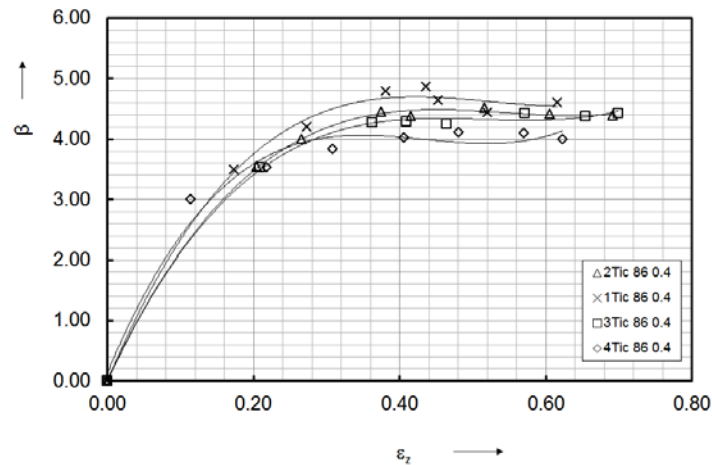

Fig. 12. Relationship between formability stress index and true height strain for various sintered aluminium composites.

Experimental data obtained during the hot deformation of TiC containing aluminium composite has been utilized to plot fracture strain (ε_z^f) and formability stress index at fracture (β^f) as shown in Fig. 13. It can be observed that the height strain at fracture increases with the increasing percentage of TiC content in the composites, however, the formability of the material is reduced. This plot can be utilized in the design of preform geometry and die constraints at the free surface of the deforming preform.
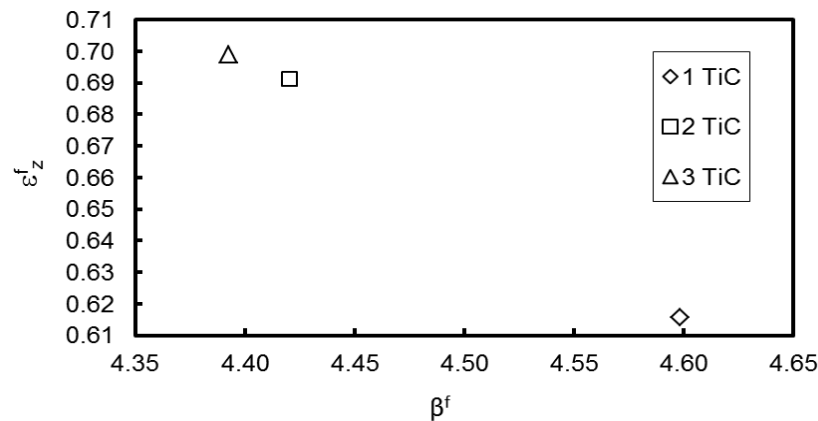
Fig. 13. Relationship between true height strain at fracture and formability stress index at fracture for various sintered aluminium composites.

Figure 14 show the optical micrographs of hot forged aluminium composites containing 1%, 2%, 3% and 4% TiC particles along the upsetting direction. Upon increasing the TiC content in the composite, the interparticle spacing between the powders decreases and the matrix grains change from elongated to equi-axed form. With the increasing TiC particles in the aluminium composite preforms, the particles have axis of approximately same length, thus more planes on which to slip promoting strength in the preform. Further, the elongated particles are frequently observed 45 degrees along the upsetting direction as the material undergoes lateral deformation along with axial (upsetting) deformation. Figure 15 show the microstructure of material consisting of 3% TiC at 100X magnification. The presence of porosity at the centre was little in comparison to extreme diametric end. Further, the pores present at the centre have round shape whilst the pores at extreme diametric side are elongated in the direction of metal flow. It can be said that effective closure of pores of a cylindrical preform at the centre is much higher in comparison to extreme diametric side.
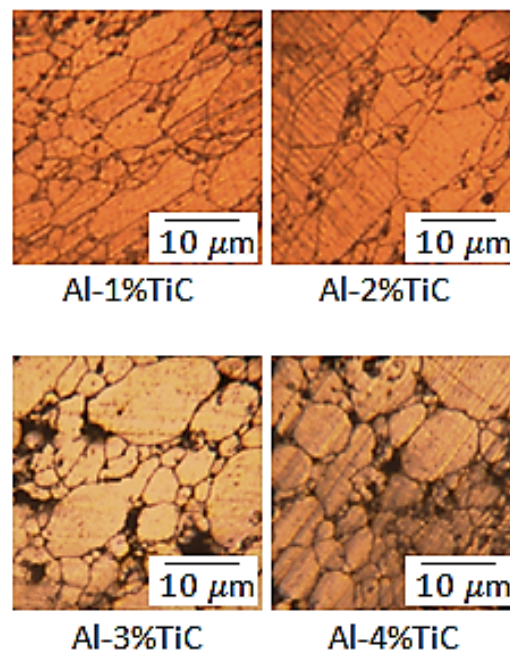

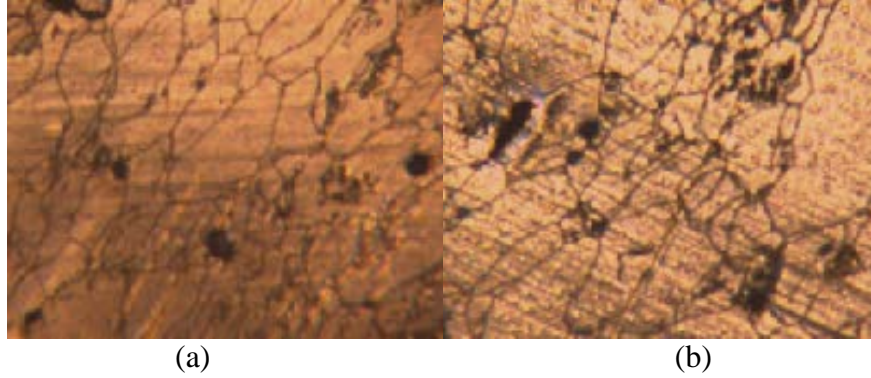**Fig. 14.** Optical micrographs of various sintered aluminium composites.

(a)   (b)

Fig. 15. (a) and (b): Optical micrographs at centre and diametric extreme of the preform, respectively.

5. Conclusions

The design of preform shape and die are very important such that the final part produced is free from defects (fracture) since there is little possibility that the cracks can be arrested during the repressing stage of the deformation. Accordingly, the major conclusions have been drawn that are as follows.

The increase in the addition of TiC content decreases the densification thereby the stress formability index of the preform.

Decreasing the aspect ratio and increasing the initial theoretical density facilitates uniform deformation resulting in improved densification and formability behavior of the preform, however, limits the height strain to fracture.

The variation of aspect ratio, initial theoretical density and TiC content in the preform made nil impact in the stress ratio behavior against densification, however, against true axial strain induced is prominent.

The increase in the addition of TiC content decreases the interparticle spacing and the matrix grains change from elongated to equi-axed form.

Notation

ε_θ	True hoop strain
ε_z	True axial strain
ε_z^f	True axial strain to fracture
ε_{eff}	Effective strain
σ_z	Axial stress
σ_θ	Hoop stress
σ_r	Radial stress
σ_m	Hydrostatic stress
σ_{eff}	Effective stress
β	Stress formability factor
β^f	Stress formability factor at fracture
R	Relative density
α	Poisson's ratio
$d\varepsilon_\theta$	Plastic hoop strain increment
$d\varepsilon_z$	Plastic axial strain increment

References

[1] J. Mascarenhas // *Materials Science Forum* **455** (2004) 857.

[2] Powder metallurgy – Intrinsically Sustainable (Metal Powder Industries Federation, 105 College Road East, Princeton, New Jersey).

[3] R.M. German Powder Metallurgy Science (MPIF, Princeton, New Jersey, USA, 1994).

[4] R.H. Derakhshandeh, A.J. Jahromi // *Materials & Design* **32** (2011) 3377.

[5] Y. Sahin // *Materials & Design* **24** (2003) 671.

[6] R. Narayanasamy, V. Senthilkumar, K.S. Pandey // *Materials Science and Engineering: A* **456** (2007) 180.

[7] Y. Liu, L.F. Chen, H.P. Tang, C.T. Liu, B. Liu, B.Y. Huang // *Materials Science and Engineering: A* **418** (2006) 25.

[8] M.C. Butuc, J.J. Gracio, B.A. Rocha // *International Journal of Mechanical Sciences* **48** (2006) 414.

[9] R. Narayanasamy, T. Ramesh, K.S. Pandey // *Materials Science and Engineering: A* **391** (2005) 418.

[10] M.A. Rahman, M.N. El-Sheikh // *Journal of Materials Processing Technology* **54** (1995) 97.

[11] R. Narayanasamy, V. Anandakrishnan, K.S. Pandey // *Materials & Design* **29** (2008) 1582.

[12] S. Shima, M. Oyane // *International Journal of Mechanical Sciences* **18** (1976) 285.

[13] A.L. Gurson // *Journal of Engineering Materials and Technology* **99** (1977) 2.

[14] S.M. Doraivelu, H.L. Gegel, J.S. Gunasekara, J.C. Malas, J.T. Morgan // *International Journal of Mechanical Sciences* **26** (1984) 527.

[15] R. Narayanasamy, T. Ramesh, K.S. Pandey // *Materials & Design* **27** (2006) 566.

[16] R. Narayanasamy, R. Ponalagusamy, K.R. Subramanian // *Journal of Materials Processing Technology* **110** (2001) 182.

[17] H.A. Kuhn, C.L. Downey // *The International journal of powder metallurgy & powder technology* **10** (1974) 59.

[18] B.B. Hwang, S. Kobayashi // *International Journal of Machine Tools and Manufacture* **30** (1990) 309.

[19] B.P.P.A. Gouveia, J.M.C. Rodrigues, P.A.F. Martins // *Journal of Materials Processing Technology* **101** (2000) 52.

[20] S.V.S. Narayanamurti, B.R. Nageswara, B.P. Kashyap // *Journal of Materials Processing Technology* **147** (2004) 94.

[21] V. Vujovic, A.H. Shabaik // *Journal of Engineering Materials and Technology* **108** (1986) 245.

[22] A. Rajeshkannan // *Materials Research* **13** (2010) 457.